EUROPEAN ORGANIZATION FOR NUCLEAR RESEARCH

First measurement of transverse-spin-dependent azimuthal asymmetries in the Drell-Yan process

Abstract

The first measurement of transverse-spin-dependent azimuthal asymmetries in the pion-induced Drell-Yan (DY) process is reported. We use the CERN SPS 190 GeV/c π^- beam and a transversely polarized ammonia target. Three azimuthal asymmetries giving access to different transverse-momentum-dependent (TMD) parton distribution functions (PDFs) are extracted using dimuon events with invariant mass between 4.3 GeV/c^2 and 8.5 GeV/c^2. The observed sign of the Sivers asymmetry is found to be consistent with the fundamental prediction of Quantum Chromodynamics (QCD) that the Sivers TMD PDFs extracted from DY have a sign opposite to the one extracted from semi-inclusive deep-inelastic scattering (SIDIS) data. We present two other asymmetries originating from the pion Boer-Mulders TMD PDFs convoluted with either the nucleon transversity or pretzelosity TMD PDFs. These DY results are obtained at a hard scale comparable to that of a recent COMPASS SIDIS measurement and hence allow unique tests of fundamental QCD universality predictions.

PACS: 13.60.-r; 13.60.Hb; 13.88.+e; 14.20.Dh; 14.65.-q

The COMPASS Collaboration

M. Aghasyan[25], R. Akhunzyanov[7], M.G. Alexeev[27], G.D. Alexeev[7], A. Amoroso[27,28], V. Andrieux[29,21], N.V. Anfimov[7], V. Anosov[7], A. Antoshkin[7], K. Augsten[7,19], W. Augustyniak[30], A. Austregesilo[16], C.D.R. Azevedo[1], B. Badełek[31], F. Balestra[27,28], M. Ball[3], J. Barth[4], R. Beck[3], Y. Bedfer[21], J. Bernhard[13,10], K. Bicker[16,10], E. R. Bielert[10], R. Birsa[25], M. Bodlak[18], P. Bordalo[12,a], F. Bradamante[24,25], A. Bressan[24,25], M. Büchele[9], W.-C. Chang[22], C. Chatterjee[6], M. Chiosso[27,28], I. Choi[29], S.-U. Chung[16,b], A. Cicuttin[26,25], M.L. Crespo[26,25], S. Dalla Torre[25], S.S. Dasgupta[6], S. Dasgupta[24,25], O.Yu. Denisov[28,#], L. Dhara[6], S.V. Donskov[20], N. Doshita[33], Ch. Dreisbach[16], W. Dünnweber[c], M. Dziewiecki[32], A. Efremov[7,s], P.D. Eversheim[3], M. Faessler[c], A. Ferrero[21], M. Finger[18], M. Finger jr.[18], H. Fischer[9], C. Franco[12], N. du Fresne von Hohenesche[13,10], J.M. Friedrich[16], V. Frolov[7,10], E. Fuchey[21,d], F. Gautheron[2], O.P. Gavrichtchouk[7], S. Gerassimov[15,16], J. Giarra[13], F. Giordano[29], I. Gnesi[27,28], M. Gorzellik[9,n], A. Grasso[27,28], M. Grosse Perdekamp[29], B. Grube[16], T. Grussenmeyer[9], A. Guskov[7], D. Hahne[4], G. Hamar[24,25], D. von Harrach[13], F.H. Heinsius[9], R. Heitz[29], F. Herrmann[9], N. Horikawa[17,e], N. d'Hose[21], C.-Y. Hsieh[22,f], S. Huber[16], S. Ishimoto[33,g], A. Ivanov[27,28], Yu. Ivanshin[7,s], T. Iwata[33], V. Jary[19], R. Joosten[3], P. Jörg[9], E. Kabuß[13], A. Kerbizi[24,25], B. Ketzer[3],G.V. Khaustov[20], Yu.A. Khokhlov[20,h,i], Yu. Kisselev[7], F. Klein[4], J.H. Koivuniemi[2,29], V.N. Kolosov[20], K. Kondo[33], K. Königsmann[9], I. Konorov[15,16], V.F. Konstantinov[20], A.M. Kotzinian[27,28], O.M. Kouznetsov[7], Z. Kral[19], M. Krämer[16], P. Kremser[9], F. Krinner[16], Z.V. Kroumchtein[7,*], Y. Kulinich[29], F. Kunne[21], K. Kurek[30], R.P. Kurjata[32], A. Kveton[19], A.A. Lednev[20,*], M. Levillain[21], S. Levorato[25], Y.-S. Lian[22,k], J. Lichtenstadt[23], R. Longo[27,28], A. Maggiora[28], A. Magnon[29], N. Makins[29], N. Makke[25,26], G.K. Mallot[10,#], B. Marianski[30], A. Martin[24,25], J. Marzec[32], J. Matoušek[25,18], H. Matsuda[33], T. Matsuda[14], G.V. Meshcheryakov[7], M. Meyer[29,21], W. Meyer[2], Yu.V. Mikhailov[20], M. Mikhasenko[3], E. Mitrofanov[7], N. Mitrofanov[7], Y. Miyachi[33], A. Nagaytsev[7], F. Nerling[13], D. Neyret[21], J. Nový[19,10], W.-D. Nowak[13], G. Nukazuka[33], A.S. Nunes[12], A.G. Olshevsky[7], I. Orlov[7], M. Ostrick[13], D. Panzieri[28,l], B. Parsamyan[27,28,#], S. Paul[16], J.-C. Peng[29], F. Pereira[1], M. Pešek[18], D.V. Peshekhonov[7], N. Pierre[13,21], S. Platchkov[21], J. Pochodzalla[13], V.A. Polyakov[20], J. Pretz[4,j], M. Quaresma[12], C. Quintans[12], S. Ramos[12,a], C. Regali[9], G. Reicherz[2], C. Riedl[29], N.S. Rogacheva[7], M. Roskot[18], D.I. Ryabchikov[20,i], A. Rybnikov[7], A. Rychter[32], R. Salac[19], V.D. Samoylenko[20], A. Sandacz[30], C. Santos[25], S. Sarkar[6], I.A. Savin[7,s], T. Sawada[22], G. Sbrizzai[24,25], P. Schiavon[24,25], K. Schmidt[9,n], H. Schmieden[4], K. Schönning[10,m], E. Seder[21], A. Selyunin[7], L. Silva[12], L. Sinha[6], S. Sirtl[9], M. Slunecka[7], J. Smolik[7], A. Srnka[5], D. Steffen[10,16], M. Stolarski[12], O. Subrt[10,19], M. Sulc[11], H. Suzuki[33,e], A. Szabelski[25,30], T. Szameitat[9,n], P. Sznajder[30], M. Tasevsky[7], S. Tessaro[25], F. Tessarotto[25], A. Thiel[3], J. Tomsa[18], F. Tosello[28], V. Tskhay[15], S. Uhl[16], A. Vauth[10], J. Veloso[1], M. Virius[19], J. Vondra[19], S. Wallner[16], T. Weisrock[13], M. Wilfert[13], J. ter Wolbeek[9,n], K. Zaremba[32], P. Zavada[7], M. Zavertyaev[15], E. Zemlyanichkina[7,s], N. Zhuravlev[7], and M. Ziembicki[32]

[1] University of Aveiro, Dept. of Physics, 3810-193 Aveiro, Portugal

[2] Universität Bochum, Institut für Experimentalphysik, 44780 Bochum, Germany[o,p]

[3] Universität Bonn, Helmholtz-Institut für Strahlen- und Kernphysik, 53115 Bonn, Germany[o]

[4] Universität Bonn, Physikalisches Institut, 53115 Bonn, Germany[o]

[5] Institute of Scientific Instruments, AS CR, 61264 Brno, Czech Republic[q]

[6] Matrivani Institute of Experimental Research & Education, Calcutta-700 030, India[r]

[7] Joint Institute for Nuclear Research, 141980 Dubna, Moscow region, Russia[s]

[8] Universität Erlangen–Nürnberg, Physikalisches Institut, 91054 Erlangen, Germany[o]

[9] Universität Freiburg, Physikalisches Institut, 79104 Freiburg, Germany[o,p]

[10] CERN, 1211 Geneva 23, Switzerland

[11] Technical University in Liberec, 46117 Liberec, Czech Republic[q]

[12] LIP, 1000-149 Lisbon, Portugal[t]

13 Universität Mainz, Institut für Kernphysik, 55099 Mainz, Germany[o]

14 University of Miyazaki, Miyazaki 889-2192, Japan[u]

15 Lebedev Physical Institute, 119991 Moscow, Russia

16 Technische Universität München, Physik Dept., 85748 Garching, Germany[o,c]

17 Nagoya University, 464 Nagoya, Japan[u]

18 Charles University in Prague, Faculty of Mathematics and Physics, 18000 Prague, Czech Republic[q]

19 Czech Technical University in Prague, 16636 Prague, Czech Republic[q]

20 State Scientific Center Institute for High Energy Physics of National Research Center 'Kurchatov Institute', 142281 Protvino, Russia

21 IRFU, CEA, Université Paris-Saclay, 91191 Gif-sur-Yvette, France[p]

22 Academia Sinica, Institute of Physics, Taipei 11529, Taiwan[v]

23 Tel Aviv University, School of Physics and Astronomy, 69978 Tel Aviv, Israel[w]

24 University of Trieste, Dept. of Physics, 34127 Trieste, Italy

25 Trieste Section of INFN, 34127 Trieste, Italy

26 Abdus Salam ICTP, 34151 Trieste, Italy

27 University of Turin, Dept. of Physics, 10125 Turin, Italy

28 Torino Section of INFN, 10125 Turin, Italy

29 University of Illinois at Urbana-Champaign, Dept. of Physics, Urbana, IL 61801-3080, USA[x]

30 National Centre for Nuclear Research, 00-681 Warsaw, Poland[y]

31 University of Warsaw, Faculty of Physics, 02-093 Warsaw, Poland[y]

32 Warsaw University of Technology, Institute of Radioelectronics, 00-665 Warsaw, Poland[y]

33 Yamagata University, Yamagata 992-8510, Japan[u]

According to Quantum Chromodynamics (QCD), the modern theory of strong interactions, the internal structure of hadrons explored in hard (semi-)inclusive scattering is described by parton distribution functions (PDFs). For a polarized nucleon, within the twist-2 approximation there are eight transverse-momentum-dependent (TMD) PDFs describing the distributions of longitudinal and transverse momenta of partons and their correlations with nucleon and quark polarizations. Experimentally, these PDFs can be accessed in the Drell-Yan process, *i.e.* massive lepton-pair production in hadron-nucleon collisions ($hN \to \ell\bar{\ell}X$), hereafter referred to as DY, and in semi-inclusive hadron measurements in deep-inelastic lepton-nucleon scattering ($\ell N \to \ell' hX$), hereafter referred to as SIDIS. For recent reviews see *e.g.* Refs. [1, 2, 3]. For the DY and SIDIS cross sections, TMD factorization was proven to hold [4], which allows one to express them as convolutions of hard-scale dependent TMD PDFs, perturbatively calculable parton hard-scattering cross sections and (for SIDIS) parton fragmentation functions. The hard scale Q in DY is given by the invariant mass of the lepton pair and in SIDIS by the square root of the virtuality of the photon exchanged in the DIS process.

The Sivers function [5] plays an important role among the TMD PDFs. It describes the left-right asymmetry in the distribution of unpolarized partons in the nucleon with respect to the plane spanned by the momentum and spin vectors of the nucleon. One of the recent significant theoretical advances in the TMD framework of QCD is the prediction that the two naively time-reversal odd TMD PDFs, *i.e.* the quark Sivers functions $f_{1T}^{\perp}$ and Boer-Mulders functions $h_1^{\perp}$, have opposite sign when measured in SIDIS or DY [6, 7, 8]. The experimental test of this fundamental prediction, which is a direct consequence of QCD gauge invariance, is a major challenge in hadron physics.

Non-zero quark Sivers TMD PDFs have been extracted from SIDIS single-differential results of HERMES [9], COMPASS [10, 11, 12, 13] and JLab [14] using both collinear [15, 16] and TMD evolution approaches [17, 18, 19, 20, 21]. The first measurement of the Sivers effect in W and Z-boson production in collisions of transversely polarized protons at RHIC was reported by the STAR collaboration [22]; the hard scales of these measurements is $Q \approx 80$ GeV/c and 90 GeV/c. It is quite different from the one explored in fixed-target experiments where Q ranges approximately between 1 GeV/c and 9 GeV/c. Hence it is not excluded that TMD evolution effects may play a substantial role when describing the STAR results using Sivers TMD PDFs extracted from fixed-target SIDIS results.

The COMPASS experiment at CERN [23, 24] has the unique capability to explore the transverse-spin structure of the nucleon in a similar kinematic region by two alternative experimental approaches, *i.e.* SIDIS and DY, using mostly the same setup. This offers the opportunity of minimizing uncertainties of TMD evolution in the comparison of the Sivers TMD PDFs when extracted from these two measurements to test the opposite-sign prediction by QCD.

Recently, COMPASS published the first multi-differential results of the Sivers asymmetry, which were extracted from SIDIS data at four different hard scales [25]. In particular for the range 4 GeV/$c < Q < 9$ GeV/c, the Sivers asymmetry for positive hadrons was found to be above zero by 3.2 standard deviations of the total experimental accuracy. This hard scale range is very similar to the one used in this Letter to analyze the DY process.

When the polarizations of the produced leptons are summed over, the general expression for the cross section of pion-nucleon DY lepton-pair production off a transversely polarized nucleon comprises five transverse spin-dependent asymmetries (TSAs), including the Sivers TSA [24, 26]. Those three TSAs that can be described by contributions from only twist-2 TMD PDFs will be addressed in this Letter. The corresponding part of the differential cross section can be written as follows:

$$\frac{d\sigma}{dq^4 d\Omega} \propto \hat{\sigma}_U \left\{ 1 + S_T \left[D_1 A_T^{\sin\varphi_S} \sin\varphi_S \right. \right.$$
$$+ D_2 \left(A_T^{\sin(2\varphi_{CS}-\varphi_S)} \sin(2\varphi_{CS}-\varphi_S) \right.$$
$$\left. \left. \left. + A_T^{\sin(2\varphi_{CS}+\varphi_S)} \sin(2\varphi_{CS}+\varphi_S) \right) \right] \right\}. \tag{1}$$

Here, q is the four-momentum of the exchanged virtual photon and $\hat{\sigma}_U = \left(F_U^1 + F_U^2 \right) \left(1 + \lambda \cos^2\theta_{CS} \right)$, with F_U^1, F_U^2 being the polarization and azimuth-independent structure functions, and the polar asymmetry λ is given as $\lambda = \left(F_U^1 - F_U^2 \right) / \left(F_U^1 + F_U^2 \right)$. At leading order of perturbative QCD, within the twist-2 approximation, $F_U^2 = 0$ and therefore $\lambda = 1$. The subscript $(U)T$ denotes transverse polarization (in)dependence. In analogy to SIDIS, the virtual-photon depolarization factors are defined as $D_1 = (1 + \cos^2\theta_{CS})/ \left(1 + \lambda \cos^2\theta_{CS} \right)$ and $D_2 = \sin^2\theta_{CS}/ \left(1 + \lambda \cos^2\theta_{CS} \right)$. The angles φ_{CS}, θ_{CS} and Ω, the solid angle of the lepton, are defined in the Collins-Soper frame as defined in Refs. [24, 26], and φ_S is the azimuthal angle of the direction of the nucleon polarization in the target rest frame, see Fig. 1.

The TSAs A_T^w in Eq. (1) are defined as amplitudes of a given azimuthal modulation $w = w(\varphi_S, \varphi_{CS})$, divided by the spin and azimuth-independent part of the DY cross section and the corresponding depolarization factor.

In this analysis, the sign convention for TSAs is given by Eq. (1) together with the definitions of azimuthal and polar angles in Fig. 1. Note that the sign of the Sivers TSA is related to that of the Sivers TMD PDF only by convention, so that the above mentioned sign-change prediction for the Sivers TMD PDFs in our case results in the same sign of the measured Sivers TSAs in SIDIS and DY.

In DY lepton-pair production with a transversely polarized nucleon in the initial state, the TSA $A_T^{\sin\varphi_S}$ is related to the nucleon Sivers TMD PDFs ($f_{1T}^\perp$) convoluted with the unpolarized pion TMD PDFs ($f_{1,\pi}$). The other two TSAs, $A_T^{\sin(2\varphi_{CS}-\varphi_S)}$ and $A_T^{\sin(2\varphi_{CS}+\varphi_S)}$, are related to convolutions of the Boer-Mulders TMD PDFs ($h_{1,\pi}^\perp$) of the pion with the nucleon TMD PDFs transversity (h_1) and pretzelosity ($h_{1T}^\perp$), respectively [26, 27]. All three aforementioned nucleon TMD PDFs induce analogous twist-2 TSAs in the general expression for the cross section of unpolarized-hadron production in SIDIS of leptons off transversely polarized nucleons [26, 27, 28]. These TSAs were studied by the HERMES and COMPASS experiments [9, 11, 12, 13, 25, 29, 30, 31, 32, 33, 34]. In contrast to the Sivers function, transversity
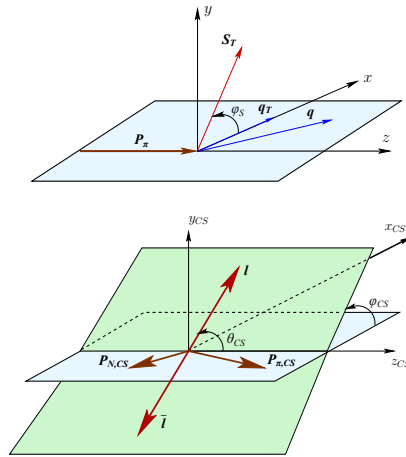

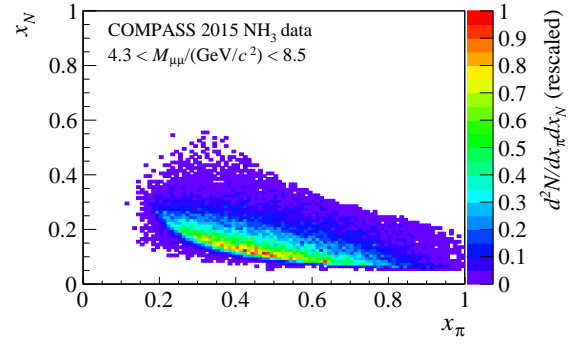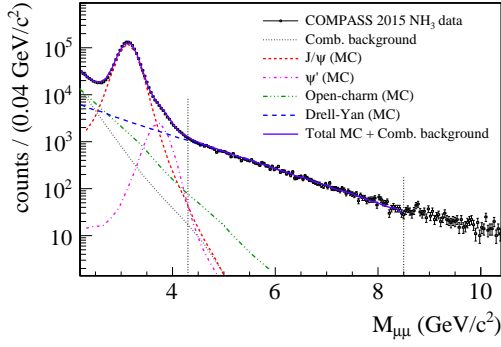Fig. 1: Top: target rest frame. Bottom: Collins-Soper frame.

Fig. 2: The dimuon invariant mass distribution.

Fig. 3: The two-dimensional (x_π, x_N) distribution of the selected high mass dimuons. The distribution is normalized to have a maximum value equal to one.

and pretzelosity are predicted to be genuinely universal, *i.e.* they do not change sign between SIDIS and DY [4], which is yet another fundamental QCD prediction to be explored.

The analysis presented in this Letter is based on Drell-Yan data collected by COMPASS in the year 2015 using essentially the same spectrometer as it was used during SIDIS data taking in previous years [23]. For this measurement, the 190 GeV/c π^- beam with an average intensity of 0.6×10^8 s^{-1} from the CERN SPS was scattered off the COMPASS transversely polarized NH$_3$ target with proton polarization $\langle P_T \rangle \approx 0.73$ and dilution factor $\langle f \rangle \approx 0.18$, where the latter accounts for the fraction of polarizable nucleons in the target and the migration of reconstructed events from one target cell to the other. The polarized target, placed in a 0.6 T dipole magnet, consisted of two longitudinally aligned cylindrical cells of 55 cm length and 4 cm in diameter, separated by a 20 cm gap. The two cells were polarized vertically in opposite directions, so that data with both spin orientations were recorded simultaneously. In order to compensate for acceptance effects, the polarization was reversed every two weeks. The entire data-taking time of 18 weeks was divided into nine periods, each consisting of two consecutive weeks with opposite target polarizations. The proton polarization had a relaxation time of about 1000 hours, which was measured for each target cell in each data taking period. A 240 cm long structure made mostly of alumina with a tungsten core, placed downstream of the target, acted as hadron absorber and beam dump. Outgoing charged particles were detected by a system of tracking detectors in the two-stage spectrometer. In each stage, muon identification was accomplished by a system of muon filters.

The trigger required the hit pattern of several hodoscope planes to be consistent with at least two muon candidates originating from the target region. For any pair of candidates either both have to be detected in the first stage of the spectrometer ($25 < \theta_\mu < 160$ mrad), or one in the first and the other in the second stage ($8 < \theta_\mu < 45$ mrad).

In the data analysis, the selection of events requires a production vertex located within the polarized-target volume, with one incoming pion beam track and at least two oppositely charged outgoing particles that are consistent with the muon hypothesis, *i.e.* they crossed at least 30 radiation lengths of material along the spectrometer. The dimuon transverse momentum q_T is required to be above 0.4 GeV/c in order to obtain sufficient resolution in angular variables.

The reconstructed mass spectrum of events passing all analysis requirements is shown in Fig. 2 (in black). The J/ψ peak is clearly visible with a shoulder from the ψ(2S) resonance. The contributions to the dimuon spectrum are evaluated with a Monte-Carlo (MC) simulation. The Drell-Yan process is shown in blue (long dashed) together with background processes: i) charmonia in red (dashed) and magenta (dot-dashed) and ii) semi-muonic open-charm decays shown in green (double dot dashed). In addition, the combinatorial background originating from the decays of pions and kaons produced in the target is evaluated using like-sign dimuon events from real data and shown in grey (dotted). The sum of
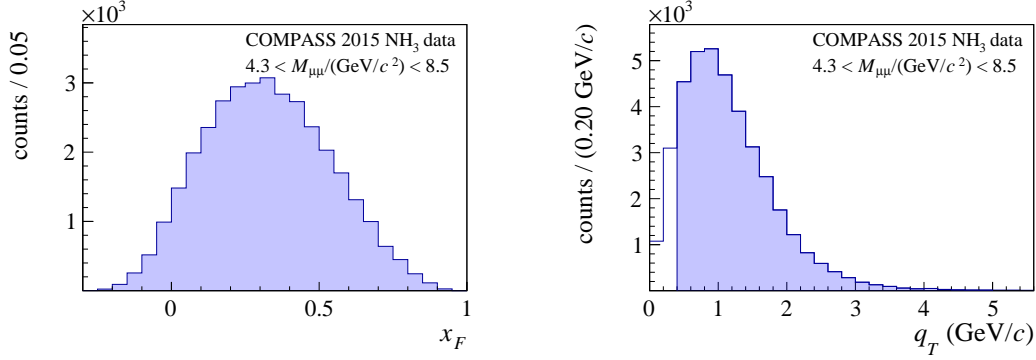
Fig. 4: The x_F distribution (left) and q_T distribution (right) of the selected high mass dimuons.

all contributions, shown in violet, describes the experimental data well. For the analysis we use the mass range 4.3 GeV/$c^2 < M_{\mu\mu} <$ 8.5 GeV/c^2, where the upper limit avoids the contribution of Υ-resonances. In this range, the sum of all background contributions is estimated to be below 4%.

The two-dimensional distribution of the Bjorken scaling variables of pion and nucleon, x_π and x_N, for this mass range is presented in Fig. 3. The figure shows that the kinematic phase space explored by the COMPASS spectrometer matches the valence region in x_π and x_N. In this region, the DY cross section for a proton target is dominated by the contribution of nucleon u-quark and pion $\bar{u}$-quark TMD PDFs.

The distributions of the dimuon Feynman variable x_F and the dimuon transverse momentum q_T are presented in Fig. 4. The corresponding mean values of the kinematic variables are: $\langle x_N \rangle = 0.17$, $\langle x_\pi \rangle = 0.50$, $\langle x_F \rangle = 0.33$, $\langle q_T \rangle = 1.2$ GeV/c and $\langle M_{\mu\mu} \rangle = 5.3$ GeV/c^2.

About 35×10^3 dimuons remain for the analysis. The three TSAs presented in this Letter are extracted period by period from the number of dimuons produced in each cell for the two directions of the target polarization. The double-cell target configuration in conjunction with the periodic polarization reversal allows for the simultaneous measurement of azimuthal asymmetries for both target spin orientations, thereby compensating flux and acceptance-dependent systematic uncertainties. Using an extended Un-binned Maximum Likelihood estimator as described in Ref. [31], all five TSAs are fitted simultaneously together with their correlation matrices. The final asymmetries are obtained by averaging the results of the nine periods. The asymmetries are evaluated in kinematic bins of x_N, x_π, x_F or q_T, while always integrating over all the other variables.

The dilution factor f and the depolarization factors D_1 and D_2 entering the definition of TSAs are calculated on an event-by-event basis and used to weight the asymmetries. For the magnitude of the target polarization P_T, an average value is used for each data taking period in order to avoid possible systematic bias. In the evaluation of the depolarization factors, the approximation $\lambda = 1$ is used. Known deviations from this assumption with λ ranging between 0.5 and 1 [35, 36] lead to a normalization uncertainty of at most -5%.

The TSAs resulting from different periods are checked for possible systematic effects. The largest systematic uncertainty is due to possible residual variations of experimental conditions within a given period. They are quantified by evaluating various types of false asymmetries in a similar way as described in Refs. [12, 30]. The systematic point-to-point uncertainties are found to be about 0.7 times the statistical uncertainties. The normalization uncertainties originating from the uncertainties on target polarization (5%) and dilution factor (8%) are not included in the quoted systematic uncertainties.

The TSAs $A_T^{\sin\varphi_S}$, $A_T^{\sin(2\varphi_{CS}-\varphi_S)}$ and $A_T^{\sin(2\varphi_{CS}+\varphi_S)}$ are shown in Fig. 5 as a function of the variables x_N, x_π, x_F and q_T. Due to relatively large statistical uncertainties, no clear trend is observed for any of the TSAs. The full set of numerical values for all TSAs including correlation coefficients and mean kinematic
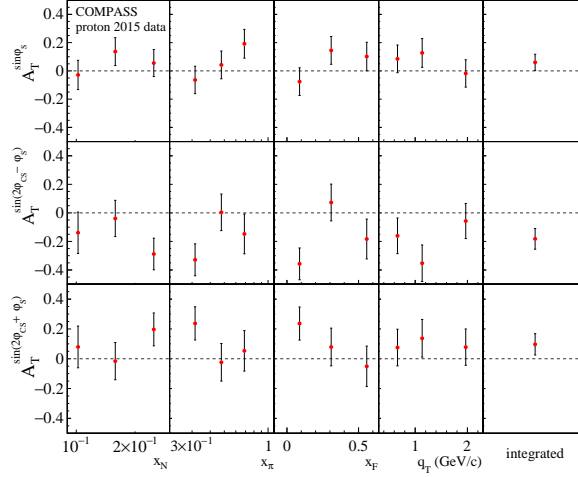
Fig. 5: Extracted Drell-Yan TSAs related to Sivers, transversity and pretzelosity TMD PDFs (top to bottom). Error bars represent statistical uncertainties. Systematic uncertainties (not shown) are 0.7 times the statistical ones.
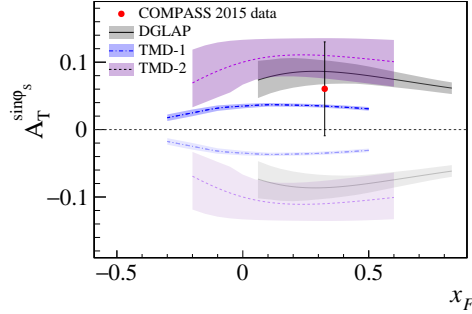

Fig. 6: The measured mean Sivers asymmetry and the theoretical predictions for different Q^2 evolution schemes from Refs. [19] (DGLAP), [20] (TMD1) and [21] (TMD2). The dark-shaded (light-shaded) predictions are evaluated with (without) the sign-change hypothesis. The error bar represents the total experimental uncertainty.

values from this measurement is available on HepData [37]. The last column in Fig. 5 shows the results for the three extracted TSAs integrated over the entire kinematic range. The average Sivers asymmetry $A_T^{\sin \varphi_S}$ is found to be above zero at about one standard deviation of the total uncertainty. In Fig. 6, it is compared with recent theoretical predictions from Refs. [19, 20, 21] that are based on different Q^2-evolution approaches. The positive sign of these theoretical predictions for the DY Sivers asymmetry was obtained by using the sign-change hypothesis for the Sivers TMD PDFs, and the numerical values are based on a fit of SIDIS data for the Sivers TSA [9, 11, 12]. The figure shows that this first measurement of the DY Sivers asymmetry is consistent with the predicted change of sign for the Sivers function.

The average value for the TSA $A_T^{\sin(2\varphi_{CS}-\varphi_S)}$ is measured to be below zero with a significance of about two standard deviations. The obtained magnitude of the asymmetry is in agreement with the model calculations of Ref. [38] and can be used to study the universality of the nucleon transversity function. The TSA $A_T^{\sin(2\varphi_{CS}+\varphi_S)}$, which is related to the nucleon pretzelosity TMD PDFs, is measured to be above zero with a significance of about one standard deviation. Since both $A_T^{\sin(2\varphi_{CS}-\varphi_S)}$ and $A_T^{\sin(2\varphi_{CS}+\varphi_S)}$ are related to the pion Boer-Mulders PDFs, the obtained results may be used to study this function further and to possibly determine its sign. They may also be used to test the sign change of the nucleon Boer-Mulders TMD PDFs between SIDIS and DY as predicted by QCD [6, 7, 8], when combined with other past and future SIDIS and DY data related to target-spin-independent Boer-Mulders asymmetries [39, 40, 41].

References

[1] M. Grosse Perdekamp and F. Yuan, Ann. Rev. Nucl. Part. Sci. **65**, 429 (2015), arXiv:1510.06783 [hep-ph] .

[2] J.-C. Peng and J.-W. Qiu, Prog. Part. Nucl. Phys. **76**, 43 (2014), arXiv:1401.0934 [hep-ph] .

[3] C. A. Aidala, S. D. Bass, D. Hasch, and G. K. Mallot, Rev. Mod. Phys. **85**, 655 (2013), arXiv:1209.2803 [hep-ph] .

[4] J. Collins, *Foundations of perturbative QCD* (Cambridge University Press, 2013).

[5] D. W. Sivers, Phys. Rev. **D41**, 83 (1990).

[6] J. C. Collins, Phys. Lett. **B536**, 43 (2002), arXiv:hep-ph/0204004 [hep-ph] .

[7] S. J. Brodsky, D. S. Hwang, and I. Schmidt, Phys. Lett. **B530**, 99 (2002), arXiv:hep-ph/0201296 [hep-ph] .

[8] S. J. Brodsky, D. S. Hwang, and I. Schmidt, Nucl. Phys. **B642**, 344 (2002), arXiv:hep-ph/0206259 [hep-ph] .

[9] A. Airapetian *et al.* (HERMES collaboration), Phys. Rev. Lett. **103**, 152002 (2009), arXiv:0906.3918 [hep-ex] .

[10] E. S. Ageev *et al.* (COMPASS), Nucl. Phys. **B765**, 31 (2007), arXiv:hep-ex/0610068 [hep-ex] .

[11] M. Alekseev *et al.* (COMPASS collaboration), Phys. Lett. **B673**, 127 (2009), arXiv:0802.2160 [hep-ex] .

[12] C. Adolph *et al.* (COMPASS collaboration), Phys. Lett. **B717**, 383 (2012), arXiv:1205.5122 [hep-ex] .

[13] C. Adolph *et al.* (COMPASS collaboration), Phys. Lett. **B744**, 250 (2015), arXiv:1408.4405 [hep-ex] .

[14] X. Qian *et al.* (Jefferson Lab Hall A), Phys. Rev. Lett. **107**, 072003 (2011), arXiv:1106.0363 [nucl-ex] .

[15] M. Anselmino, M. Boglione, U. D'Alesio, A. Kotzinian, F. Murgia, and A. Prokudin, Phys. Rev. **D72**, 094007 (2005).

[16] M. Anselmino, M. Boglione, U. D'Alesio, A. Kotzinian, S. Melis, F. Murgia, A. Prokudin, and C. Turk, Eur. Phys. J. **A39**, 89 (2009), arXiv:0805.2677 [hep-ph] .

[17] S. M. Aybat, A. Prokudin, and T. C. Rogers, Phys. Rev. Lett. **108**, 242003 (2012), arXiv:1112.4423 [hep-ph] .

[18] M. Anselmino, M. Boglione, and S. Melis, Phys. Rev. **D86**, 014028 (2012), arXiv:1204.1239 [hep-ph] .

[19] M. Anselmino, M. Boglione, U. D'Alesio, F. Murgia, and A. Prokudin, (2016), arXiv:1612.06413 [hep-ph] .

[20] M. G. Echevarria, A. Idilbi, Z.-B. Kang, and I. Vitev, Phys. Rev. **D89**, 074013 (2014), arXiv:1401.5078 [hep-ph] .

[21] P. Sun and F. Yuan, Phys. Rev. **D88**, 114012 (2013), arXiv:1308.5003 [hep-ph] .

[22] L. Adamczyk *et al.* (STAR collaboration), Phys. Rev. Lett. **116**, 132301 (2016), arXiv:1511.06003 [nucl-ex] .

[23] P. Abbon *et al.* (COMPASS collaboration), Nucl. Instrum. Meth. **A577**, 455 (2007), arXiv:hep-ex/0703049 [hep-ex] .

[24] F. Gautheron *et al.* (COMPASS collaboration), SPSC-P-340, CERN-SPSC-2010-014 (2010).

[25] C. Adolph *et al.* (COMPASS), (2016), arXiv:1609.07374 [hep-ex] .

[26] S. Arnold, A. Metz, and M. Schlegel, Phys. Rev. **D79**, 034005 (2009), arXiv:0809.2262 [hep-ph] .

[27] A. Bacchetta, M. Diehl, K. Goeke, A. Metz, P. J. Mulders, and M. Schlegel, JHEP **02**, 093 (2007), arXiv:hep-ph/0611265 [hep-ph] .

[28] A. Kotzinian, Nucl. Phys. **B441**, 234 (1995), arXiv:hep-ph/9412283 [hep-ph] .

[29] C. Adolph *et al.* (COMPASS), Phys. Lett. **B736**, 124 (2014), arXiv:1401.7873 [hep-ex] .

[30] C. Adolph *et al.* (COMPASS collaboration), Phys. Lett. **B717**, 376 (2012), arXiv:1205.5121 [hep-ex] .

[31] C. Adolph *et al.* (COMPASS collaboration), Phys. Lett. **B713**, 10 (2012), arXiv:1202.6150 [hep-ex] .

[32] B. Parsamyan (COMPASS collaboration), *Proceedings, 20th International Symposium on Spin Physics (SPIN 2012)*, Phys. Part. Nucl. **45**, 158 (2014), arXiv:1301.6615 [hep-ex] .

[33] L. L. Pappalardo (HERMES collaboration), in *Exclusive reactions at high momentum transfer. Proceedings, 4th Workshop, Newport News, USA, May 18-21, 2010* (2011) pp. 312–320.

[34] F. Bradamante (COMPASS), in *22nd International Symposium on Spin Physics (SPIN 2016) Urbana, IL, USA, September 25-30, 2016* (2017) arXiv:1702.00621 [hep-ex] .

[35] M. Guanziroli *et al.* (NA10), Z. Phys. **C37**, 545 (1988).

[36] J. S. Conway *et al.*, Phys. Rev. **D39**, 92 (1989).

[37] HepData (The Durham HepData Project), (2016).

[38] A. N. Sissakian, O. Yu. Shevchenko, A. P. Nagaitsev, and O. N. Ivanov, Phys. Part. Nucl. **41**, 64 (2010).

[39] S. Falciano *et al.* (NA10), Z. Phys. **C31**, 513 (1986).

[40] A. Airapetian *et al.* (HERMES), Phys. Rev. **D87**, 012010 (2013), arXiv:1204.4161 [hep-ex] .

[41] C. Adolph *et al.* (COMPASS), Nucl. Phys. **B886**, 1046 (2014), arXiv:1401.6284 [hep-ex] .